Gramicidin channel selectivity

Molecular mechanics calculations for formamidinium, guanidinium, and acetamidinium

Brian Turano, Michael Pear, and David Busath
Section of Physiology and Biophysics, Brown University, Providence, Rhode Island 02912 USA

ABSTRACT Empirical energy function calculations were used to evaluate the effects of minimization on the structure of a gramicidin A channel and to analyze the energies of interaction between three cations (guanidinium, acetamidinium, formamidinium) and the channel as a function of position along the channel axis. The energy minimized model of the gramicidin channel, which was based on the results of Venkatachalam and Urry (1983), has a constriction at the channel entrance. If the channel is not allowed to relax in the presence of the ions (rigid model), there is a large potential energy barrier for all three cations. The barrier varies with cation size and is due to high van der Waals and ion deformation energies. If the channel is minimized in the presence of the ions, the potential energy barrier to formamidinium entry is almost eliminated, but a residual barrier remains for guanidinium and acetamidinium. The residual barrier is primarily due, not to the expansion of the helix, but, to the disruption of hydrogen bonds between the terminal ethanoloamine and the next turn of the helix which occurs when the carbonyls of the outer turn of the helix librate inward toward the ion as it enters the channel. The residual potential energy barriers could be a possible explanation for the measured selectivity of gramicidin for formamidinium over guanidinium. The results of this full-atomic model address the applicability of the size-exclusion concept for the selectivity of the gramicidin channel.

INTRODUCTION

Size-exclusion has been suggested as one possible mechanism of ion channel selectivity (e.g., Hille, 1971, 1992; Bezanilla and Armstrong, 1972). Selective channels are thought to have a narrow selectivity filter region along the permeation reaction coordinate which forces ion dehydration and poses a steric barrier to permeant ions. The size-exclusion principle states that ions which are too big to pass through the narrow filter are impermeant. For instance, the observation that the sodium channel is permeable to guanidinium but not methylguanidinium has been interpreted to mean that the sodium channel has a 3×5 Å selectivity filter, narrow enough to exclude methylguanidinium but not guanidinium (Hille, 1975). To test the size-exclusion concept we use a channel of known structure and pose the question: if the structure of a channel is known, can the size-exclusion principle predict accurately which ions can and cannot penetrate the channel? More generally, it is necessary to determine whether steric (van der Waals repulsion) terms are most important. Also, it is essential to consider whether the channel can be considered as a rigid pore or whether flexibility plays a role in allowing ions to permeate.

We use Gramicidin A for which better structural data are available than for more biologically relevant systems. Gramicidin A channels are cation-selective pores formed in lipid bilayers by head-to-head dimers of a 15-residue peptide twisted in a $\pi_{L,D}$ helix (Andersen, 1984; Pullman, 1987; Cornell, 1987). The helical twist was initially inferred to be left-handed (Urry et al., 1982) but is now thought to be right-handed (Arseniev et al., 1985, 1986; Nicholson and Cross, 1989; Andersen et al., 1990). Calculations indicate that the interior of the ion channel is very similar whether it is left- or right-handed (Venkatachalam and Urry, 1983). The calculations reported here were done with a left-handed helix, but are expected to be representative for the right-handed helix as well.

The channel has 6.3 amino acids per turn (Urry, 1971; Popov and Lipkind, 1979; Arseniev et al., 1985, 1986; Naik and Krimm, 1986*a,b;* Cornell et al., 1988; Nicholson and Cross, 1989). The internal diameter was first estimated to be about 4 Å (Urry, 1971) and later as 3.7 Å, based on coordinates from molecular mechanics and the "hard-core" atomic radii[1] (Busath et al., 1988).

Guanidinium and similar organic cations are well suited as probes of the gramicidin channel interior dimensions. The permeability to guanidinium is <0.027 P_K according to reversal potentials of multichannel membranes (Eisenman et al., 1976) and the single channel conductance is <0.004 γ_K (Busath et al., 1988). The permeability to formamidinium is >1.55 P_K (Eisenman et al., 1976). Both molecules are flat (all atoms are co-

Please send correspondence to Dr. David Busath, Box G, Brown University, Providence, RI 02912.

[1] For the hard core radius, r, a variant of the Lennard-Jones equation is used to predict the atom surface that would not be entered more than ~5% of the time by other atoms in thermal conditions (electrostatic interactions are neglected):

$$r = R_{min}\left[\frac{E_m + [E_m(E_m - E_v)]^{1/2}}{E_v}\right]^{1/6} \quad E_m < 0 < E_v.$$

R_{min} is the van der Waals radius, E_m is the van der Waals energy for the atom when its center is located $2R_{min}$ away from the center of the same type of atom, and E_v is a cutoff energy, above which the atom is unlikely to be found. When E_v is 1.8 kcal/mol, ($3RT$ for $T = 300$ K), $r =$ 0.75, 0.78, 0.80, and 0.72 R_{min} for C, O, N, and H, respectively. The values used for E_m (kcal/mol) and R_{min} (Å) are −0.0903, −0.1591, −0.2384, −0.0498 and 1.9, 1.8, 1.6, 0.8, respectively (Brooks et al., 1983).

0006-3495/92/07/152/10 $2.00

planar) due to a resonating double bond. The silhouettes have heights of 4.9 Å (Busath et al., 1988) and 3.9 Å, respectively, using the hard-core dimensions. Thus, guanidinium would be too large to fit through the 3.7 Å gramicidin channel according to the size-exclusion theory, whereas formamidinium (which would also be unable to fit through the channel if the walls were rigid) is a closer match to the channel diameter.

We use these ions as probes to examine the size-exclusion concept more carefully, taking into account the complexity of the real molecular surface and the full interaction energy, instead of the steric interactions alone. Furthermore, guanidinium causes blocks in potassium-mediated currents which get shorter with increased membrane potential, suggesting that guanidinium can permeate the channel, albeit rarely (Busath et al., 1988; Hemsley and Busath, 1991). (If the block rate reflects the guanidinium transport rate, the permeability to guanidinium is $\sim 10^6$ times lower than formamidinium.) Acetamidinium causes similar blocks (Hemsley and Busath, 1991) and appears from the block rate to be more than an order of magnitude less permeant than guanidinium. These findings stimulated the study presented here.

A previous report (Busath et al., 1988) examined the fit of guanidinium through a model gramicidin channel that was minimized using quenched molecular dynamics. Here the analysis is extended using a gramicidin structure that was minimized using a staged, Adopted-basis Newton-Raphson (ABNR) minimization method (Brooks et al., 1983). Also, two other organic cations, formamidinium and acetamidinium, are compared with guanidinium. In both reports, a left-handed $\beta^{6.3}$ structure was used. As in the previous study, we compare results between a rigid and flexible channel as a function of ion position. No solvent was included in the calculations. Although this is clearly a severe limitation, particularly for electrostatic energy analyses, it is of less importance for the van der Waals interactions, which are of primary concern for the size-exclusion model. In the previous report, we found that a constriction at the channel entry/exit caused a large energy barrier to guanidinium entry that was largely relieved when the channel is free to adjust to the ion. The importance of flexibility for protein function is well established for larger proteins such as hemoglobin (Frauenfelder et al., 1979; Case and Karplus, 1979). The possibility that freedom of the COOH-terminal ethanolamine in gramicidin was important to alkali metal cation entry was explored and eventually discounted by Pullman and co-workers (Etchebest et al., 1984; Etchebest and Pullman, 1986; Trudelle et al., 1987). Molecular dynamics computations indicate that the mobility of the water chain in a gramicidin channel is dramatically increased when the channel is flexible, indicating that peptide librations contribute to water flow through the channel (Chiu et al., 1991). Here we observe that for guanidinium and acetamidinium, consistent with experimental observations, a residual potential energy barrier to entry remains after channel labilization and we discuss its origin and energy composition.

COMPUTATIONAL METHOD

Gramicidin model

The gramicidin A model was constructed with the program CHARMM (Brooks et al., 1983). The total energy was computed as the sum of bond length, bond angle, torsion angle, improper torsion angle, electrostatic, and van der Waals terms as described elsewhere. Electrostatic and van der Waals energy calculations were truncated at 7.5 Å by use of a switching function. The electrostatic energy was computed with a constant dielectric coefficient, $\epsilon = 1$. Hydrogen bonds arise from the electrostatic interactions due to the assignment of partial charges to polar hydrogens (W. Reiker and M. Karplus, unpublished data). Aliphatic hydrogens not involved in hydrogen bonding were modeled implicitly using extended carbon atoms. The model for the gramicidin A monomer initially contained 157 atoms and later, with the addition of an explicit formyl hydrogen to better simulate the head-to-head docking, 158 atoms. D-amino acids required redefinition of the alpha carbon chirality; the improper dihedral angle was modified from 120° to −120°. Ethanolamine and formyl terminator residues were modeled after the standard CHARMM residues, serine and acetyl, respectively. Bond parameters were from Brooks et al. (1983) except for the C—C—O bond of ethanolamine, which we assigned to be 111° with force constant 45.0 kcal/mol-rad^2.

Initial estimates for the peptide ϕ, ψ, χ_1, and χ_2 angles and monomer docking parameters came from the Venkatachalam and Urry (1983) conformational analysis for the left-handed single-stranded head-to-head docked $\beta^{6.3}$ helices (their Table III) which we refer to as the VU structure. The peptide dihedral angle conventions used by Venkatachalam and Urry were identical to the standard residue dihedrals defined in the CHARMM topology file (the TOPH19 version was used here) except for the Trp χ_2 which differs by 180° and was therefore defined explicitly. The VU dihedrals for the left-handed helix are similar to the dihedrals recommended by Popov and Lipkind (1979) for their helix number 7 and by Koeppe and Kimura (1984). The principle problems with the VU structure, when generated using the present force field, were repulsive van der Waals contacts between Val^7 and Trp^{13} side chains, Trp^9 and Leu^{10} side chains, and formyl hydrogens at the dimer junction.

In an earlier study (Busath et al., 1988), a 157-atom monomer was constructed using the dihedral angles from Venkatachalam and Urry (1983), visually oriented along the x-axis, and duplicated to obtain a symmetric dimer. Optimal docking parameters for the two monomers were determined using an energy-contour map for the monomer separation versus relative axial rotation. The docked dimer was energy minimized by quenched dynamics. It was first heated from 0° to 300° K over 4 ps by scaling the velocities, cooled to ~0° K over 4 ps, and finally energy minimized for 1,000 steps. The final structure had an RMS energy derivative of 11.73 kcal/Å. We refer to this structure as the MDQ (molecular dynamics quench) dimer. Data for the energy of interaction of the MDQ dimer with guanidinium were given in the prior report (Fig. 5, in Busath et al., 1988).

In this paper we give results for similar computations done with a second gramicidin model, the SM (staged minimization) dimer. For the SM dimer, the structure was minimized starting from the 158-atom VU monomer in five stages. Each stage was carried out with fewer constraints on the peptide components. The side chain for Val^7 was found to be in contact with Trp^{13} in the initial structure. Changing χ_1 for Val^7 from 60° to 170° eliminated this contact and reduced the van der Waals energy for the monomer from 1,134 to 101 kcal/mol. Next, the positions of all atoms were fixed except for the side chains of 7, 9, 10, and 13 which were harmonically constrained to their initial values, and energy minimized using 10 steps of the ABNR algorithm (Brooks et al., 1983). Then the positions of only the backbone atoms were fixed,

TABLE 1

Residue	Staged minimization ϕ	Staged minimization ψ	M.D. quench ϕ	M.D. quench ψ
1 Val	−148.38	136.39	−108.16	105.61
3 Ala	−144.14	119.19	−131.14	115.78
5 Ala	−137.87	126.02	−135.26	118.15
7 Val	−123.44	122.65	−124.50	113.60
9 Trp	−120.22	126.39	−121.09	112.67
11 Trp	−135.24	130.12	−116.91	126.24
13 Trp	−144.66	137.02	−135.17	124.81
15 Trp	−152.75	115.12	−138.96	104.58
2 Gly	120.92	−125.76	112.18	−121.51
4 D-Leu	111.72	−131.80	111.23	−123.17
6 D-Val	109.48	−133.31	111.70	−133.49
8 D-Val	104.36	−130.02	121.63	−131.59
10 D-Leu	100.99	−116.94	112.67	−123.47
12 D-Leu	93.00	−99.07	89.09	−97.73
14 D-Leu	78.51	−92.33	88.46	−106.54
Docking parameters				
d (Angstroms)	1.4		2.4	
θ (degrees)	129.8		129.0	

and the side chain positions were further minimized using 1,000 steps of steepest descents. Two copies of the minimized monomer were oriented with the principle elliptical axis of their backbone atoms on the x-axis, docked using the parameters recommended by Venkatachalam and Urry (1983), and minimized with all atoms free using 1,000 steps of steepest descents. The final conformation had an RMS energy derivative of 1.51 kcal/Å. The MDQ and SM dimers were then both realigned with the center of the channel at the origin and the primary elliptical axis of the peptide backbone atoms (the channel axis) on the x-axis.

The backbone dihedral angles for the SM and MDQ methods (Table 1) are similar to the VU angles for the D-amino acids and to the Koeppe and Kimura (1984) angles for the L-amino acids, except at the COOH-terminal where the constriction occurs. The variations in ϕ and ψ are similar to those reported by Roux and Karplus (1988) for an independently minimized channel structure. The average values (Table 2) are similar to those used previously (helix 7 from Popov and Lipkind, 1979; Venkatachalam and Urry, 1983; Koeppe and Kimura, 1984; Roux and Karplus, 1988). In a preliminary study (data not shown), molecular dynamics quenching of gramicidin starting from the Koeppe and Kimura (1984) dihedrals yielded average backbone dihedral angles within 3° of the averages for the MDQ dimer (which was started from the VU configuration). This indicates that the MDQ conformation is accessible from either the Koeppe and Kimura or VU starting points during dynamics. Basically, the differences between these structures are minor as far as the conclusions of this paper are concerned.

TABLE 2

	ϕL	ψL	ϕD	ψD
Backbone dihedrals				
VU	−144	132	104	−118
KK	−133	116	120	−130
PL7	−109	123	141	−129
Average backbone dihedrals				
SM	−138.3	126.6	102.7	−118.5
MDQ	−126.4	115.2	106.7	−119.6
RK	−135.0	129.6	96.8	−112.9

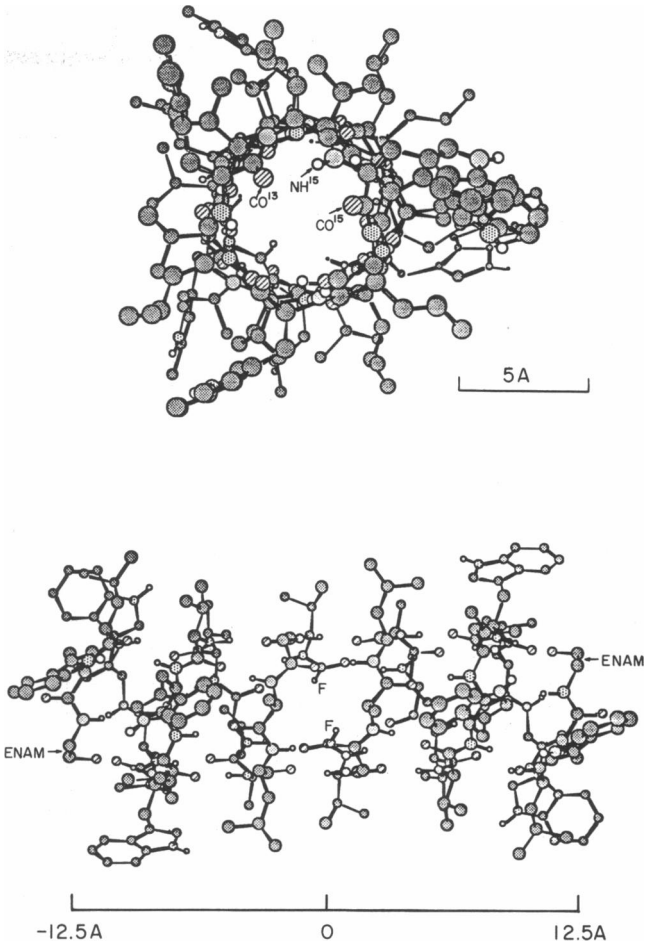

FIGURE 1 Gramicidin dimer obtained using a staged minimization of the VU dimer (see text). Carbon: gray; polar hydrogen: white; nitrogen: stippled; oxygen: striped. (*Top*) End-on view showing the intrusion of carbonyl oxygens from Trp-13 and Trp-15 and the amide hydrogen from Trp-15 into the channel. The view is orthogonal with depth-cuing by atom size so that the intrusive atoms at the distant end appear as very small circles. (*Bottom*) Side view. F: formyl; Enam: ethanolamine.

The constriction at the mouth of the channel is a result of peptide libration (Venkatachalam and Urry, 1984; Roux and Karplus, 1988). The carbonyl of amino acid i librates into the channel without significant displacements of the alpha carbons or side chains if ψ_i is increased and ϕ_{i+1} is decreased by the same amount. We found that for the SM and MDQ structures, ψ^{13} is abnormally large (137°, SM) and ϕ^{14} is small (79°, SM), causing the inward rotation of CO^{13} seen in Fig. 1. Also, NH^{15}, CO^{15}, and other backbone atoms from the outer turn of the helix help to constrict the channel pathway (Fig. 1).

The docking parameters (Table 1; defined in Venkatachalam and Urry, 1983) were similar to those used previously (Venkatachalam and Urry, 1983). The SM side chain dihedrals (Table 3) were similar to the VU dihedrals except for χ_2 of D-Leu^4, Trp^9, and Trp^{15} and χ_1 of Val^7. Those of the MDQ dimer are more randomized, as expected for a structure minimized by quenched dynamics. We do not expect the side chain dihedrals or docking parameters to affect the conclusions of this paper. The total dimer energy (Table 4) was lower for the SM dimer than for the MDQ dimer due to the more extensive minimization, and both were much lower than the unminimized VU dimer. The docking energy (Table 4) is the potential energy of the docked dimer less that of the pair of (otherwise unmodified) monomers separated.

TABLE 3 **Side chain positions (degrees)**

	VU		SM		MDQ	
Residue	χ_1	χ_2	χ_1	χ_2	χ_1	χ_2
1 Val	60.		61.27		−175.63	
4 D-Leu	180.	120.	178.33	170.96	179.01	173.40
6 D-Val	62.		54.42		171.25	
7 Val	60.		176.59		−174.69	
8 D-Val	63.		55.36		173.81	
9 Trp	176.	−60.	−179.05	−101.67	−167.57	−84.92
10 D-Leu	60.	58.	68.29	64.78	167.42	176.05
11 Trp	180.	62.	−175.58	56.81	171.13	−121.31
12 D-Leu	60.	60.	68.61	65.98	165.58	174.66
13 Trp	178.	59.	−165.02	62.68	173.07	−120.61
14 D-Leu	60.	63.	67.25	67.06	168.54	172.92
15 Trp	177.	57.	165.77	−87.77	−149.92	−81.22

Cation models

The organic cation structures were derived by changing the amide that connects the guanidino group from the standard CHARMM arginine to the rest of the side chain. For guanidinium, the amide was disconnected from the side chain carbon which was replaced by a hydrogen atom (CHARMM atom type HC). For formamidinium and acetamidinium, the amide was replaced with an aliphatic hydrogen (atom type HA) and an extended-carbon type of methyl group (atom type CH3E), respectively. The bond lengths, bond angles, dihedral and improper dihedral angles, and their force constants were all defined in the standard CHARMM parameter set (Brooks et al., 1983), except for the following additions, which were based on similarity to other standard parameters: for formamidinium, HA—C—N 118°, 40 kcal/mol-rad^2; for acetamidinium, CH3E—C—N 118°, 65 kcal/mol-rad^2; and for guanidinium, C—N—N—N (the improper dihedral that controls out-of-plane bending), 0°, 100 kcal/mol-rad^2. For acetamidinium and formamidinium, the partial charge for each atom was the same as in the arginine guanidinium group in the CHARMM topology file (TOPH19): H, 0.35; N, −0.45; and C, 0.5. The aliphatic hydrogen in formamidinium and extended-carbon methyl in acetamidinium were each assigned a zero charge. For guanidinium, partial charges from the self-consistent field calculations of Herzig et al. (1981) were used: H, 0.435; N, −0.918; and C, 1.141. These guanidinium partial charges may be somewhat too large and would lead to an overestimate of the favorable electrostatic interaction energy between the guanidinium ion and the channel. However, they would not affect the van der Waals energy, which is most important for the entry barrier when the channel is fixed, nor the electrostatic gramicidin energy, which dominates when the channel is free.

Calculations

The energy minimizations done with guanidinium in the MDQ dimer were described previously (Busath et al., 1988). The computations with the SM dimer were similar but more thorough. For each ion, two series of energy minimizations were done with the ion constrained to positions along the x-axis, the axis of the SM dimer. For convenience, the ion was constrained by fixing the central carbon to the x-axis and leaving the remaining atoms of the ion free. In the first series of calculations, the gramicidin atoms were fixed. The ion was minimized with 100 steps of ABNR algorithm with the central carbon at positions between x = −4.0 Å and x = 20.0 Å at 0.05-Å intervals. In the second series of calculations, the flexibility of the channel entrance (which presents the highest energy barrier to ion translation) was ascertained by removing the constraints on either the entire nearby monomer or on residues 9–15 and the ethanolamine terminus of the nearby monomer. The remainder of the channel was fixed in each case to prevent channel translation. The ion was then minimized for positions between x = 8.0 Å and x = 15.0 Å at 0.05-Å intervals. The relative system energy was computed as the total system energy with the ion at a given position minus the total system energy with the ion outside of the unmodified SM dimer channel (x = 90 Å). This procedure subtracts out the covalent bonding energy and nonbonded interactions of the fixed part of the channel structure (actually, nonbonded interactions between fixed atoms are excluded from the energy calculation in the first place) and allows one to focus on the nonbonded interactions between the ion and the channel, and on the covalent bonding energy of the ion alone (channel fixed) or of the ion and the mobile part of the channel (channel partially fixed). The relative electrostatic, van der Waals, and covalent bonding energies were computed in the same way.

To identify all local minima, six different ion starting angles were used in the minimizations. The ion was oriented so that the plane of the ion contained the channel axis. The ion starting angle was defined as the angle, ϕ_0, between the plane of the ion and the vector from the origin to the midpoint between the two formyl carbons at the center of the channel. For each x, minimizations were performed with ϕ_0 ranging from 0° to 150° in increments of 30°; considering the bilateral symmetry of the ions, the entire circumference of the channel was explored in this way. The six different starting positions resulted in 1 to 3 (most often 2) different final positions, indicating that results of the minimization could be sensitive to the starting position of the ion. The global minimum was used without regard for its proximity to the orientation of the ion at the adjacent grid points.

TABLE 4 **Dimer energy**

	VU	SD	MDQ
		kcal/mol	
van der Waals	2987.3	−122.1	−120.8
Electrostatic	−779.5	−900.7	−865.5
Internal	137.1	148.8	200.4
Total	2344.8	−874.0	−785.9
Docking energy	710.5	−54.1	−54.5

RESULTS

The structure of the gramicidin dimer after the staged minimization, SM, is shown in Fig. 1. At the center of the channel, the hard core internal diameter is equal to 3.6 Å, similar to that of the VU channel. However, the

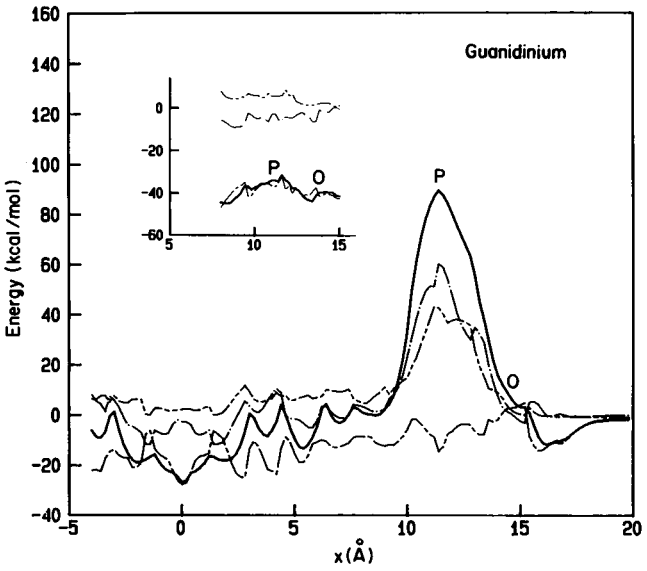

FIGURE 2 Guanidinium-gramicidin channel minimum relative system energy as a function of distance from the center of the channel with the gramicidin channel fixed in space parallel to the x-axis and the ion carbon fixed on the x-axis. The channel entrances are at $x = \pm 12.5$ Å. Calculations were performed for the entire positive x region; 4 Å in the negative x region were also analyzed to demonstrate the symmetry of the channel. (——) Relative system energy; (– – –) relative electrostatic energy; (– · –) relative van der Waals energy; (– – – –) relative covalent bonding energy. The total and component energies with the ion at x = 90 Å were used as the references. (*Inset*) Minimum relative energies computed as above but with residues 9–15 and ethanolamine for the monomer in the positive x region free to accommodate the ion. The negative x monomer and residues 1–8 of the positive x monomer were left fixed to anchor the channel axis on the x-axis during the minimization. The location of the energy peak (11.6 Å) is labeled p, and the point just outside the channel (14.6 Å) is labeled o.

dimer exhibits a narrowing of the channel entrance which is due to inward bending of the carbonyl oxygens of Trp[13] and Trp[15]. This constricts the entrance to a hard core diameter of 2.9 Å. Otherwise, the end-on view of the channel in Fig. 1 is similar to that of the VU structure (Venkatachalam and Urry, 1983, Fig. 4). The interior of the MDQ channel does not differ appreciably from that of SM. The internal hard core diameter of the channel is 4.0 Å in the center of the channel and 2.6 Å at the entrance.

Fig. 2 is a plot of guanidinium-gramicidin relative system energy as a function of guanidinium position on the axis of the channel. In the main figure, the SM dimer and the central guanidinium carbon were fixed as the rest of the guanidinium was energy minimized. The relative system energy (*solid line*) is negative between $x = 0.0$ Å (the center of the channel) and $x = 10.0$ Å, and has a large peak near the mouth of the channel at $x = 12.5$ Å. There is a peak in total energy at $x = 11.4$ Å, which results from high relative van der Waals energy and relative covalent bonding energy. The relative covalent bonding energy is due entirely to the guanidinium group and the high value indicates that the guanidinium is distorted by repulsive interactions with the channel in the constricted region. After the ion is removed from the channel ($x > 15$ Å), the relative system energy is negative, due mainly to electrostatic attraction between the ion and the channel (hydrogen bonds between guanidinium and the oxygens of carbonyls 11, 13, and 15 and ethanolamine); it becomes negligible by $x = 20$ Å. In this region outside the channel entry, shielding and hydration would be expected to reduce the attractive interactions if water and salt were included in the calculations.

The relative system energy was symmetrical about $x = 0.0$ (from −4.0 Å to 4.0 Å), as expected for the symmetric channel, providing a further check for local minima associated with the starting position of the ion. The results with the guanidinium central carbon fixed to the x-axis (used here) agree qualitatively with the previous study done with the MDQ dimer (Busath et al., 1988), where the guanidinium central carbon was fixed in its x coordinate but free to move in the y-z plane. For instance, as in Fig. 2, the energy profile for guanidinium in the fixed MDQ channel had a large barrier between $x = 9$ Å and $x = 13$ Å, with negative relative system energy throughout the rest of the channel interior. In that study, however, the peak barrier height was lower, reflecting the freedom of the ion to move slightly off axis and better reduce the repulsive van der Waals contacts.

Except at the constriction, guanidinium appears to fit in the channel in spite of its dimensions. Fig. 3 is a series of eight frames that show the positions adopted by the guanidinium as it is stepped away from the center of the channel in 0.4 Å steps along the axis between $x = 3.8$ Å and $x = 6.6$ Å. Atoms are rendered as spheres with radii of 75% van der Waals radius, approximating the hard core radius to best display prohibited contacts (Busath et al., 1988). The point of view is fixed in the center of the channel at $x = 0$ and the scene is rendered with a perspective (rather than orthographic) view that produces an illusion of channel narrowing in individual frames, but enhances depth perception when the series is viewed as a whole. The sequence demonstrates that by a series of rotations, the guanidinium is able to adopt acceptable orientations at each step.

In our calculations, the minimum energy pathway is quite irregular (in spite of the simplicity of the beta-helix structure), being governed by complex steric and hydrogen-bonding interactions. From 3 to 5 guanidinium hydrogens form hydrogen bonds with peptide carbonyl oxygens at most positions in the channel. Frames 4–7 in Fig. 3 show rotation about the C—N bond for one of the guanidinium amides. Such deformations are the source of increased covalent bonding energy at the constriction. The figure demonstrates that guanidinium could sterically fit through the channel but that the pathway would be very restricted.

The constriction and energy barrier at the entry are mostly relieved if the gramicidin atoms are free to relax

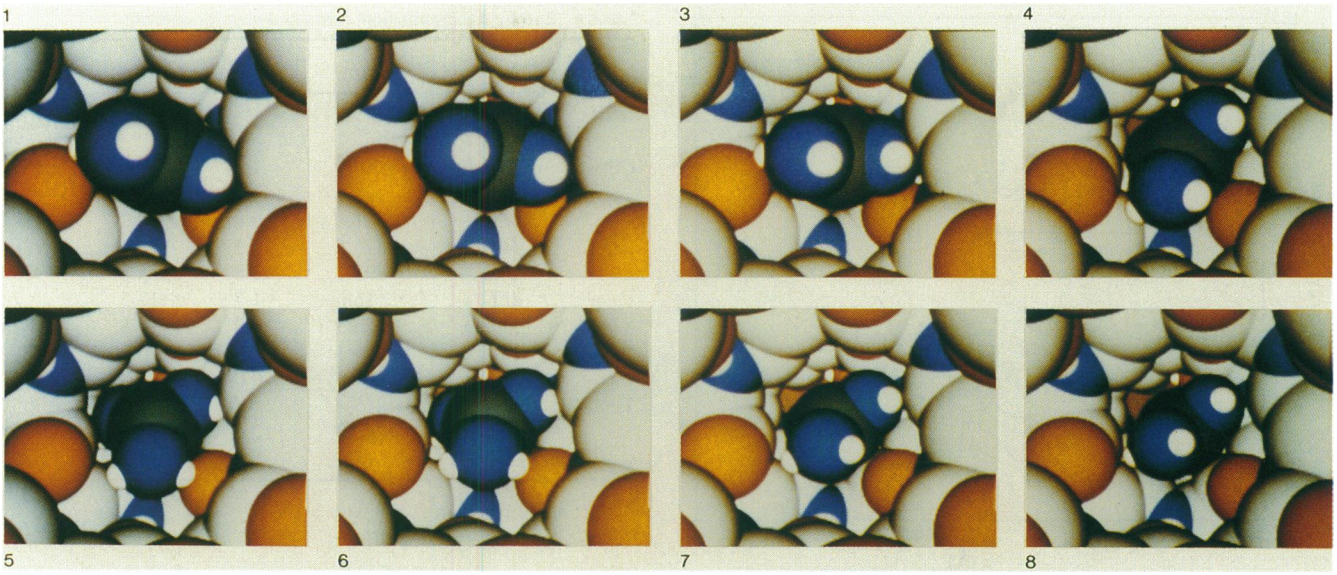

FIGURE 3 A space-filling image of guanidinium in the fixed SM gramicidin channel showing the ion's progress, as viewed from the center of the channel, from ion central-carbon positions x = 3.8 Å to x = 6.6 Å in 0.4-Å steps. Thus, as the frames progress, the channel remains unchanged and the ion is stepped further away. In each case, the minimum energy configuration is shown. All atoms are rendered as spheres with 75% of the van der Waals radius.

(*inset*, Fig. 2). The channel was fixed except for residues 9–15 and the ethanolamine for the positive x monomer. The van der Waals barrier to guanidinium passage is removed, though a residual barrier, due primarily to electrostatic and covalent contributions, remains. Between x = 14.4 Å and 11.6 Å, labeled as o (outside) and p (peak), the relative system energy rises substantially. A similar result was found in the previous study (Busath et al., 1988), where a residual barrier of ~7 kcal/mol is calculated for the guanidinium entry step from x = 11.5 Å to x = 11.0 Å.

Table 5 reports the components of the residual barrier for guanidinium. The data for this table are from a study identical to that shown in Fig. 2 except that the entire gramicidin monomer (rather than just residues 9–15 and ethanolamine) was free. This allowed for slightly improved coordination of the ion by the channel. For each component, the total energies with the ion at the peak of the barrier (11.6 Å), outside the channel (14.6 Å), and the differences between them are given. The "diff" row represents the components of the residual entry barrier on the assumption that the energy change from ∞ to 14.6 Å is negligible as it would be if solvent shielding were included in the computation. Table 5 shows that the "peak" minus "outside" difference in total system energy (the residual entry barrier) is 7.1 kcal/mol, which is comprised of destabilizing electrostatic (7.1 kcal/mol) and covalent bond (4.4 kcal/mol) contributions and stabilizing van der Waals (−4.4 kcal/mol) contributions. This is due to a large increase in total gramicidin energy (26.7 kcal/mol) compensated by improved total ion-channel interactions (−20.1 kcal/mol). The increased gramicidin energy is due primarily to electrostatic energy (22.5 kcal/mol, 84%) and bond energy (4.3 kcal/mol, 16%), whereas the improved ion-channel interactions have large electrostatic (−15.8 kcal/mol) and van der Waals (−4.3 kcal/mol) contributions. The ion itself makes a negligible contribution.

TABLE 5 **Energy decomposition: guanidinium/gramicidin**

		Gram	Guan	Inter	System
			kcal/mol		
COV	11.6 Å	158.9	2.9	0.0	161.8
	14.6 Å	154.6	2.8	0.0	157.4
	diff	4.3	0.1	0.0	4.4
ELEC	11.6 Å	−871.5	−12.0	−72.9	−956.4
	14.6 Å	−894.0	−12.4	−57.1	−963.5
	diff	22.5	0.4	−15.8	7.1
VDW	11.6 Å	−124.1	−0.6	−4.2	−128.9
	14.6 Å	−124.0	−0.6	0.1	−124.5
	diff	−0.1	0.0	−4.3	−4.4
Total	11.6 Å	−836.7	−9.7	−77.1	−923.5
	14.6 Å	−863.4	−10.2	−57.0	−930.6
	diff	26.7	0.5	−20.1	7.1

In the rows labeled "COV", the total covalent bonding energy is given for the gramicidin dimer, the guanidinium, and in the final column, the total for the entire system. The rows labeled "ELEC" contain the electrostatic energy; the "VDW" rows contain the van der Waals energy; and the "TOTAL" rows contain the sum of "COV", "ELEC", and "VDW" energies. The columns labeled "Inter" contain the "System" energy minus the sum of the "Gram" energy and the "Guan" energy for each row. This corresponds to the ion-channel interaction energy, which consists only of nonbonded ("ELEC" and "VDW") energy components. The values in the final column are each the sum of the other three values in the row; and, the values in the "Total" rows are the sums of the corresponding "COV", "ELEC", and "VDW" energies for the column. "diff": difference. See text for explanation of 11.6 Å, 14.6 Å, and "diff".

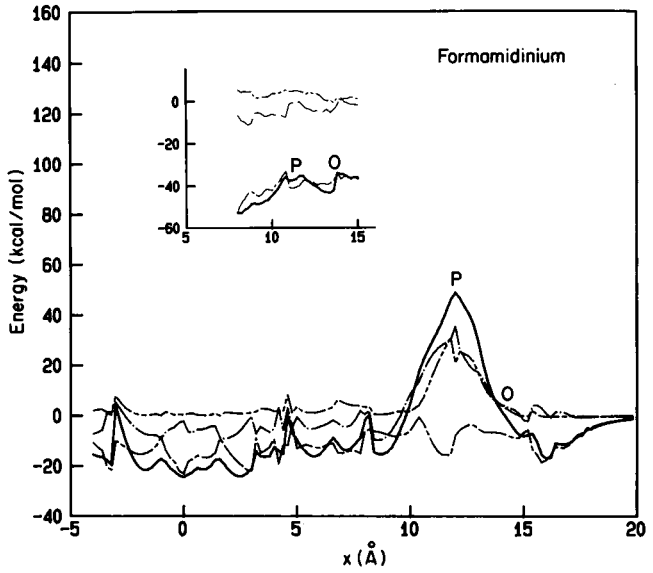

FIGURE 4 Formamidinium-gramicidin channel minimum relative energy versus distance from the center of the channel. Key as in Fig. 2.

The same protocol was used to examine the relative system energies for the SM channel and formamidinium (Fig. 4) or acetamidinium (Fig. 5). As was found with guanidinium, the relative system energy for formamidinium and acetamidinium are moderate except for a large peak at the entrance. The insets in Figs. 4 and 5 show that when the monomer is free to relax, its van der Waals repulsion is largely relieved for formamidinium and acetamidinium, as it is for guanidinium. In the case of the smaller formamidinium ion, the relief is nearly

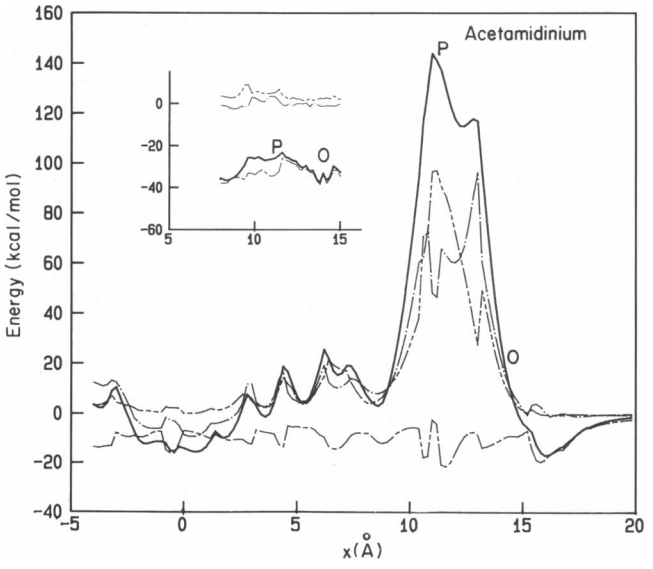

FIGURE 5 Acetamidinium-gramicidin channel minimum relative energy versus distance from the center of the channel. Key as in Fig. 2.

TABLE 6 **Energy decomposition: formamidinium/gramicidin**

		Gram	Ion	Inter	System
			kcal/mol		
COV	11.5 Å	157.4	1.9	0.0	159.3
	14.5 Å	155.6	1.1	0.0	156.8
	diff	1.8	0.8	0.0	2.5
ELEC	11.5 Å	−876.5	10.1	−72.4	−938.8
	14.5 Å	−893.1	11.8	−54.8	−936.2
	diff	16.6	−1.7	−17.5	−2.5
VDW	11.5 Å	−126.3	−0.3	0.8	−125.8
	14.5 Å	−125.3	−0.3	0.5	−125.1
	diff	−1.0	0.0	0.3	−0.7
Total	11.5 Å	−845.4	11.7	−71.6	−905.3
	14.5 Å	−862.8	12.6	−54.4	−904.5
	diff	17.4	−0.9	−17.2	−0.7

"diff": difference.

complete. Only a minor difference exists between the energy outside (o) and at the peak (p). The components of the residual barrier to ion entry (from a calculation identical to the one used for Table 5) are given for formamidinium in Table 6 and for acetamidinium in Table 7. When formamidinium is moved from 14.6 to 11.6 Å, there is an increase in total gramicidin energy (17.4 kcal/mol), but the increase is not as great as for guanidinium (26.7 kcal/mol) and for formamidinium, it is completely compensated by enhanced favorable interaction energy (−17.2 kcal/mol). There is no residual entry barrier (−0.7 kcal/mol). For acetamidinium, the residual peak is substantial (*inset,* Fig. 5). As is the case for guanidinium, the gramicidin energy increase, shown in Table 7, is greater than the interaction energy decrease and a residual barrier to entry of 6.2 kcal/mol results.

The increase in channel electrostatic energy for all three ions indicates that the residual barrier is associated with disruption of intramonomer hydrogen bonds, because they are the main source of channel electrostatic energy. This is illustrated for guanidinium in Fig. 6. The

TABLE 7 **Energy decomposition: acetamidinium/gramicidin**

		Gram	Ion	Inter	System
			kcal/mol		
COV	11.5 Å	156.9	1.5	0.0	158.3
	14.5 Å	156.0	1.8	0.0	157.8
	diff	0.9	−0.3	0.0	0.6
ELEC	11.5 Å	−878.7	11.5	−57.9	−925.1
	14.5 Å	−904.5	10.6	−35.5	−929.4
	diff	25.8	0.9	−22.5	4.2
VDW	11.5 Å	−126.1	−0.4	1.6	−124.8
	14.5 Å	−124.8	−0.4	−1.1	−126.2
	diff	−1.3	0.0	2.7	1.4
Total	11.5 Å	−847.9	12.6	−56.3	−891.6
	14.5 Å	−873.3	12.0	−36.5	−897.8
	diff	25.4	0.5	−19.8	6.2

"diff": difference.

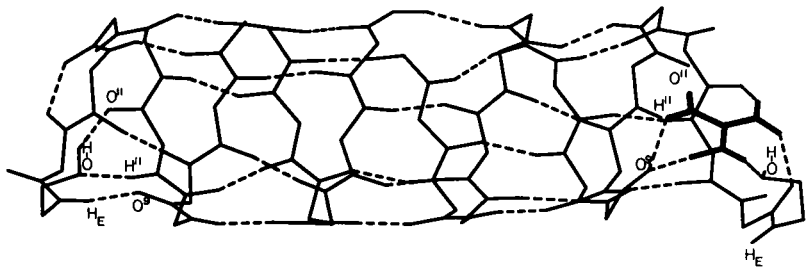

FIGURE 6 Minimized structure with guanidinium at 11.5 Å. Wire-frame view of channel backbone and ion. Dashed lines display hydrogen bonds. Hydrogen bond requirements used were: distance between hydrogen and acceptor less than 2.5 Å; distance between atom attached to hydrogen and acceptor less than 3.3 Å; angles at hydrogen, acceptor, and atom attached to hydrogen all greater than 90°. Ion in bold. The coordinates are from the same series as Table 5: right-hand monomer free, left-hand monomer fixed, ion carbon fixed to x = 11.5 during minimization.

ion (shown in bold lines) has been held at x = 11.5 Å and minimized with the entire right hand monomer (the same computation as used for Table 5). The left hand monomer is in the SM conformation. Looking first at the left hand end, it is seen that the terminal ethanolamine hydroxyl (labeled O—H) forms hydrogen bonds with the amide proton and carbonyl oxygen of Trp^{11} and the ethanolamine amide H (H_E) with the carbonyl oxygen of Trp^9. On the right hand end, the ethanolamine O and O^9 are hydrogen bonded to the guanidinium ion. H^{11}, O^{11}, and the terminal ethanolamine H form no hydrogen bonds at all. These broken hydrogen bonds in the channel, partially compensated by improved hydrogen bonds between the channel and the ion, make the dominant contributions to the residual barrier. A similar disruption occurs with acetamidinium. With formamidinium, only the ethanolamine O and H, but not the amide, break hydrogen bonds and the range in x of the disruption is smaller. Disruption of intramolecular hydrogen bonds near the gramicidin channel entry has also been described for a molecular dynamics study of hydrated sodium entry (Bobak et al., 1991).

To a lesser extent, channel (and ion) covalent bonding energy changes contribute to the residual energy barrier. These include bond stretching, angle bending, and dihedral rotation effects and are reflected in Tables 5–7 (in the entry, Gram COV diff) and the relative covalent bonding energy plotted in the insets to Figs. 2, 4, and 5. These appear to be related to the librations of the peptide backbone which relieve the constriction formed by the outer turn of the helix. The extent and sequence of these channel backbone changes for guanidinium entry is indicated in Fig. 7, where only the backbone atoms of the outer turn of the helix have been plotted for clarity. In Fig. 7 *a*, before the ion is introduced, the amide hydrogens and carbonyl oxygens of Trp^{13} and Trp^{15} are all rotated toward the channel axis. When the ion is located at 13.1 Å (Fig. 7 *b*), O^{15} moves away from the axis due to van der Waals repulsion from the ion, and H^{15} even further due to electrostatic repulsion from the ion. In Fig. 7 *c*, the ion is at the peak of the residual barrier, x = 11.6 Å. By this point, O^{15} has rotated back in toward the axis, following the cation which has passed by it (see Fig. 6). O^{13} and H^{13} have librated out due to van der Waals and electrostatic repulsion, respectively. O^{11} and H^{11} are still rotated toward the channel axis. By x = 10.1 Å (Fig. 7 *d*), O^{15} and O^{13} are strongly rotated inward, following the ion, whereas O^{11} is now rotated out due to van der Waals repulsion from the ion. H^{15} and H^{13} are still rotated out due to electrostatic repulsion. Finally, at x = 8.6 Å (Fig. 7 *e*), O^{15}, O^{13}, and O^{11} are all strongly rotated inward behind the ion and the amide hydrogens, H^{15} and H^{13}, have also adopted an inward rotation, and approach the carbonyl oxygens more closely.

DISCUSSION

The purpose of this study was to assess the simple size-exclusion model for predicting channel permeability. The computations presented here indicate that if the channel had the constricted entrance predicted by energy minimization and were rigid, the van der Waals interactions would prevent the passage of all three ions, consistent with the simple application of the size exclusion principle for guanidinium and acetamidinium, but not for formamidinium. If the channel is not artificially constrained, there is sufficient flexibility inherent in the backbone dihedrals to accommodate all three. There is still a residual energy barrier for the two larger ions, guanidinium and acetamidinium. These results are not fully consistent with the size exclusion principle, but are in qualitative accord with experiment; i.e., the residual barrier magnitudes are on the order of those suggested by their block rates.

Block rates indicate that guanidinium entry into the gramicidin channel is $\sim 10^6$ times less frequent at a given voltage than formamidinium entry, and acetamidinium entry is another order of magnitude lower (Busath et al., 1988; Hemsley and Busath, 1991). If the entry step is assumed to involve small ion motions, e.g., on the order of 2–4 Å, it is reasonable to suppose that guanidinium and acetamidinium entry is an activated process (Cooper et al., 1988) associated with a large energy barrier. Hemsley and Busath (1991) assumed that the

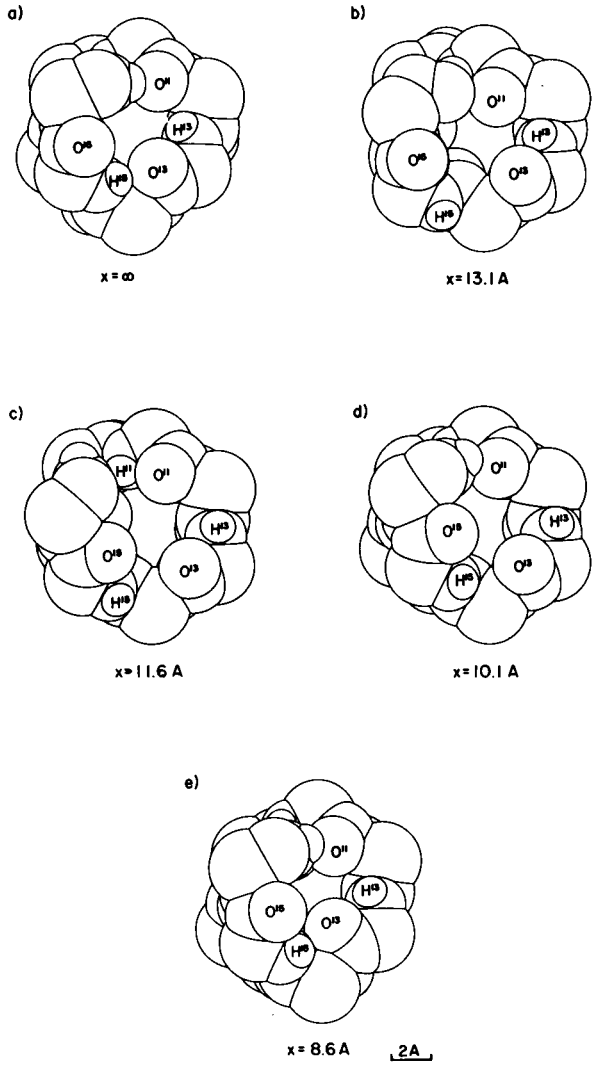

FIGURE 7 Comparison of the van der Waals views of the last turn of the gramicidin helix after minimization with the guanidinium carbon placed at the x locations specified. The coordinates are from the same series as Table 5 and Fig. 6. The side chains and the guanidinium ion are deleted for clarity. The atomic radii are plotted 5–20% smaller than the van der Waals radii used in the computation.

entry barrier for formamidinium must be negligible because the flux rate is near the diffusion-limited rate for a 4 Å pore and concluded that the activation energy for guanidinium entry is ~8.6 kcal/mol, and for acetamidinium is ~10.6 kcal/mol. These differences can be compared with the differences in residual entry barriers reported here: 7.1 kcal/mol (guanidinium) and 6.2 kcal/mol (acetamidinium). The agreement is reasonable considering the neglect of hydration and thermal motion. However, activated dynamics studies would be needed to establish the extent to which guanidinium entry is ballistic as opposed to friction limited. The low guanidinium block rate may alternatively be ascribed to increased frictional forces acting over a greater distance when molecular dynamics are taken into account.

A similar type of argument might be made about the duration of blocks, which could be expected to depend on the effective height of the barrier to exit among other things. However, this study has not addressed the nature of the residual system energy in the region of the channel interior (0–8 Å), which would be required to assess the height of the barrier to ion exit, nor do our calculations allow an estimation of the translocation rate. These topics will be left for future study.

One final consideration concerns the kinetics of the peptide motions. Could the iminium entry rate be governed not solely by the energy of peptide librations, but also by the kinetics? In the SM channel the constriction at the entry is relieved by small librational displacements of residues 11, 13, and 15. The kinetics of motion of the constriction are reflected in the normal modes of vibration of the peptide units. Roux and Karplus (1988) computed the overlap of peptide libration motions with gramicidin normal modes. Overlaps in the region of 75 to 175 cm^{-1} were predominant for peptide librations. This corresponds to frequencies of $2.25 \times 10^{12} - 5.25 \times 10^{12}$ s^{-1}, which are low frequency oscillations compared with bond stretching and bending, but are still very high compared, for instance, with the formamidinium permeation frequency at 100 mV ($\sim 5 \times 10^{7}$ s^{-1}). Since the lipid and water environment not included in the normal modes calculation have small effects on the carbonyl libration frequencies (Martin Karplus, personal communication), the relaxation kinetics of a constriction at the entrance should not limit ion entry.

We wish to thank Kevin Gaffney, John Ireland, Jeff Lefstin, Rashid Ahmad, and Sumeet Murarka for some of the calculations and figures, and Martin Karplus, Bernard Brooks, and Benoit Roux for helpful discussions.

The study was supported by NIH grants to David Busath (GM33361 and NS01085).

Received for publication 26 November 1990 and in final form 9 March 1992.

REFERENCES

Andersen, O. S. 1984. Gramicidin channels. *Annu. Rev. Physiol.* 46:531–548.

Andersen, O. S., L. L. Providence, and R. E. Koeppe. 1990. Gramicidin channels are right-handed β-helical dimers. *Biophys. J.* 57:100*a*. (Abstr.)

Arseniev, A. S., I. L. Barsukob, V. F. Bystrov, A. L. Lomize, and Y. A. Ovchinnikov. 1985. ^{1}H-NMR study of gramicidin A transmembrane ion channel. Head-head right-handed, single-stranded helices. *FEBS Lett.* 186:168–174.

Arseniev, A. S., I. L. Barsukov, and V. F. Bystrov. 1986. Conformation of gramicidin A in solution and micelles: two dimensional ^{1}H NMR study. *In* Chemistry of Peptides and Proteins. W. Voelter, E. Bayer, Y. A. Ovchinnikov, and B. T. Ivanov, editors. Walter de Gruyter/Berlin, New York. 3:127–158.

Bezanilla, F., and C. M. Armstrong. 1972. Negative conductance

caused by entry of sodium and cesium ions into the potassium channels of squid axon. *J. Gen. Physiol.* 60:588–608.

Bobak, M., S.-W. Chiu, and E. Jakobsson. 1991. Dynamic visualization of simulated motions in a membrane ion channel. *J. Mol. Graphics* 9:44–45.

Brooks, B. B., R. E. Broccoleri, B. D. Olafson, D. J. States, S. Swaminathan, and M. Karplus. 1983. CHARMM: a program for macromolecular energy, minimization and dynamics calculations. *Computational Chem.* 4:187–217.

Busath, D., G. Hemsley, T. Bridal, M. Pear, K. Gaffney, and M. Karplus. 1988. Guanidinium as a probe of the gramicidin channel interior. *In* Transport through Membranes: Carriers, Channels and Pumps. A. Pullman, J. J. Jortner, and B. Pullman, editors. Kluwer Academic Publishers, Boston. 187–201.

Case, D. A., and M. Karplus. 1979. Dynamics of ligand binding to heme proteins. *J. Mol. Biol.* 132:343–368.

Chiu, S.-W., E. Jakobsson, S. Subramaniam, and J. A. McCammon. 1991. Time-correlation analysis of simulated water motion in flexible and rigid gramicidin channels. *Biophys. J.* 60:273–285.

Cooper, K. E., P. Y. Gates, and R. S. Eisenberg. 1988. Diffusion theory and discrete rate constants in ion permeation. *J. Membr. Biol.* 106:95–105.

Cornell, B. 1987. Gramicidin A-phospholipid model systems. *J. Bioenerg. Biomembr.* 19:655–676.

Cornell, B. A., F. Separovic, A. J. Baldassi, and R. Smith. 1988. Conformation and orientation of gramicidin A in oriented phospholipid bilayers measured by solid state carbon-13 NMR. *Biophys. J.* 53:67–76.

Eisenman, G., S. Krasne, and S. Ciani. 1976. Further studies on ion selectivity. *In* Ion and Enzyme Electrodes in Medicine and in Biology. M. Kessler, L. Clark, D. Lubbers, I. Silver, and W. Simon, editors. Urban and Schwarzenberg/Munich, Berlin, Vienna. 3–22.

Etchebest, C., and A. Pullman. 1986. The gramicidin A channel. The energy profile calculated for Na^+ in the presence of water with inclusion of the flexibility of the ethanolamine tail. *FEBS Lett.* 204:261–265.

Etchebest, C., S. Ranganathan, and A. Pullman. 1984. The gramicidin A channel: comparison of the energy profiles of Na^+, K^+, and Cs^+. Influence of the flexibility of the ethanolamine end chain on the profiles. *FEBS Lett.* 173:301–306.

Frauenfelder, H., and P. G. Wolynes. 1985. Rate theories and puzzles of hemeprotein kinetics. *Science (Wash. DC).* 229:337–345.

Herzig, L., L. J. Massa, and A. Santoro. 1981. Guanidinium ion self-consistent field calculations: fluoro, amino, and methyl single substituents. *J. Org. Chem.* 46:2330–2333.

Hemsley, G., and D. Busath. 1991. Small iminium ions block gramicidin channels in lipid bilayers. *Biophys. J.* 59:901–908.

Hille, B. 1971. The permeability of the sodium channel to organic cations in myelinated nerve. *J. Gen. Physiol.* 58:599–619.

Hille, B. 1975. Ionic selectivity of Na and K channels of nerve membranes. *In* Membranes,—A Series of Advances. G. Eisenman, editor. Marcel Dekker, New York. 3:255–323.

Hille, B. 1992. Ionic Channels of Excitable Membranes. 2nd ed. Sinauer Associates, Sunderland, MD. 335–361.

Koeppe, R. E., and M. Kimura. 1984. Computer building of β-helical polypeptide models. *Biopolymers.* 23:23–38.

Naik, V. M., and S. Krimm. 1986a. Vibrational analysis of the structure of gramicidin A. I. Normal mode analysis. *Biophys. J.* 49:1131–1145.

Naik, V. M., and S. Krimm. 1986b. Vibrational analysis of the structure of gramicidin A. II. Vibrational spectra. *Biophys. J.* 49:1147–1154.

Nicholson, L. K., and T. A. Cross. 1989. The gramicidin cation channel: an experimental determination of the right-handed helix sense and verification of β-type hydrogen bonding. *Biochemistry.* 28:9379–9385.

Popov, E. M., and G. M. Lipkind. 1979. Conformational state and mechanism of the functioning of gramicidin A. *Mol. Biol.* 13:275–284.

Pullman, A. 1987. Energy profiles in the gramicidin A channel. *Quart. Rev. Biophys.* 20:173–200.

Roux, B., and M. Karplus. 1988. The normal modes of the gramicidin-A dimer channel. *Biophys. J.* 53:297–309.

Trudelle, Y., P. Daumas, F. Heitz, C. Etchebest, and A. Pullman. 1987. Experimental and theoretical study of gramicidin P, an analog of gramicidin A with a methylamine C-terminal. *FEBS Lett.* 216:11–16.

Urry, D. 1971. The gramicidin A transmembrane channel: a proposed π(L,D) helix. *Proc. Natl. Acad. Sci. USA.* 68:672–676.

Urry, D. W., J. T. Walker, and T. L. Trapane. 1982. Ion interactions in the (1-^{13}C)D-Val^8 and D-Leu^{14} analogs of gramicidin A. The helix sense of the channel and location of ion binding sites. *J. Membr. Biol.* 69:225–231.

Venkatachalam, C. M., and D. W. Urry. 1983. Theoretical conformational analysis of the gramicidin A transmembrane channel. I. Helix sense and energetics of head-to-head dimerization. *J. Comput. Chem.* 4:461–469.

Venkatachalam, C. M., and D. W. Urry. 1984. Theoretical analysis of gramicidin A transmembrane channel. II. Energetics of helical librational states of the channel. *J. Comput. Chem.* 5:64–71.